

Characterization of Copper Tailings In Murgul Copper Plant (Artvin/Turkey) And Utilization Potential In Cement Mortar With Nano And Micro Silica

İlknur BEKEM KARA (✉ ilknurbekem@artvin.edu.tr)

Artvin Çoruh Üniversitesi: Artvin Coruh Universitesi

Research Article

Keywords: Wastes of mining, copper tailings, nano silica, micro silica, mortar, strength

Posted Date: July 7th, 2021

DOI: <https://doi.org/10.21203/rs.3.rs-510906/v1>

License:   This work is licensed under a Creative Commons Attribution 4.0 International License.

[Read Full License](#)

Abstract

Due to the increasing demand for copper day by day, copper tailings (CT) are the wastes that mining and human-induced activities caused have become a problem all over the world due to the increasing demand for copper. This study evaluates the effect of using CT together with nano silica (NS) and micro silica (MS) in mortars as a partial substitution for cement on mechanical strength properties. Physical, morphological, chemical, mineralogical thermo gravimetric analyzes of CT have been made. In addition, heavy metal concentrations were determined. The mechanical features of the mortars produced by replacing by weight with different proportions of (5%, 10%, 15%) CT, 2% NS and 10% MS cement were determined. As a result, it has been observed that the sum of SiO_2 , Al_2O_3 and Fe_2O_3 of the CT, which has a mostly crystalline structure, is 91.40% and its ignition loss is 4.04%. An improvement in compressive strength (compared to the reference mixture) was observed with the use of 5% CT. Up to 10% of CT has provided standard compressive strength values in both NS and MS combinations.

Highlights

- The main chemical composition of copper tailings (CT) is SiO_2 .
- The cement in the mortar was replaced with 5%, 10% and 15% CT.
- Also, 2% nano silica (NS) and 10% micro silica (MS) were used with CT in mortar mixtures
- Up to 10% of CT has provided standard compressive strength values in both NS and MS combinations.

Introduction

The mining industry is one of the oldest human activities. The need for mining activities is growing in parallel with the world population. Copper is highly preferred in the home, industrial and high technology range due to its chemical, physical and aesthetic features (International copper study group 2020). Copper goes through the stages of "exploration, detection, preparation, ore production, enrichment and smelting" till it arrives at industrial facilities as a raw material (Sezgin 2020). The enrichment stage is removing the copper from ore to separate the economical mineral from uneconomical. At this stage, a lot of mine tailing arises. The disposal of these tailings is one of the most essential environmental problems in a copper mine. In order to prevent the uncontrolled release of copper enrichment tailings to the atmosphere; usually a dam-shaped storage facility is used (Thomas et al. 2013). However, because these tailings cover large areas of land, their toxicity and concentration or their interaction with environmental factors such as oxygen and water can cause serious environmental impacts (Lam et al. 2021). The land area occupied by waste dams is increasing day by day. Therefore, it has become an essential requirement to consume tailings in order to protect the environment and land resources (Li et al. 2020a). Studies in which copper enrichment wastes are used instead of cement and aggregate are available in the literature (Thomas et al. 2013; Dandautiya and Singh 2019; Zhang et al. 2020; Vargas et al. 2020). Because today cement and aggregate are two components that are problematic in terms of sustainability

in concrete production (Kara De Maeijer et al. 2020). The search for materials that can be used instead of cement is still ongoing, especially since the amount of energy required for cement production is high and cement is the most expensive concrete component (Xu et al. 2020; Bumanis et al. 2020; Mahadevan et al. 2021; Ogawa et al. 2021). In addition, the CO₂ emission amount of cement is among the primary reasons for environmental pollution (Padavala et al. 2021). Micro silica (MS), which is partially included in concrete as a cement substitute and is one of the most researched materials is qualified as high quality (Ni et al. 2021). It has been reported that Ca(OH)₂, which is a hydration product and damages concrete, is converted to CSH crystals with MS, and an impermeable structure is obtained by filling the gaps formed in the mortar phase of the concrete with the produced CSH crystals (Topçu and Canbaz 2008). It is also known that the deterioration of MS-containing concrete is noticeably slower than normal concrete for most chemical and physicochemical attacks (Lewis and Fidjestøl 2019).

With the developing concrete technology, while researches are directed towards alternative materials that can be substituted into cement, new materials reduced to smaller particle sizes are also tried to improve the performance of cement (Yu et al. 2020; Ma et al. 2020). In this context, the use of nano materials has been focused on in recent years to increase the strength and durability of cement composites (Shafaei et al. 2020; Li et al. 2020b; Horszczaruk et al. 2020). When we look at the materials subject to the research, it is seen that nano silica (NS) takes the first place (Kara 2020; Kooshafar and Madani 2020). According to Atmaca et al. (2017), it can be said that NS particles are very beneficial for concrete in two ways. The first is the chemical effect that the pozzolanic reaction of free Ca(OH)₂ breaks larger pores into smaller pores to form more CSH. The second is due to the physical features of NS. Smaller NS particles fill micro pores and help increase strength (Atmaca et al. 2017). This has been experimentally supported by many researchers (Snehal et al. 2020; Mukharjee and Barai 2020). It is reported that the optimum amount of NS is 2–3% (Abhilash et al. 2021).

Replacing cement with materials such as NS and MS is known to be effective in improving its mechanical properties and durability (Emamian and Eskandari-Naddaf 2020; Li et al. 2021). Yiğit et al. (2020) stated that being able to manage waste with another waste will reduce the amount of cement needed by using more waste in the mixture and will support recycling by highlighting the beneficial properties of the waste (Yiğit et al. 2020). Studies on the use of different wastes together in cement composites are available in the literature (Durgun and Sevinç 2019; Dandautiya and Singh 2019; Guo et al. 2020; Ozturk et al. 2020; Qureshi et al. 2020; Choudhary et al. 2021). To the author's knowledge, CT and MS, as well as CT and NS together, have not been substituted for cement in mortar production so far. In this context, this study focuses on the experimental determination of the effect of using CT together with MS and NS on the mechanical features in mortar production.

Materials And Methods

2.1. Murgul Copper Plant and Copper tailings

Copper mine (Fig. 1) in Murgul (Artvin / Turkey), operational since 1907 (Koz et al. 2012), and 3500000 tons of copper ore are mined and processed annually and 130000 tons of copper concentrate are produced annually (Eti Bakır 2021). Wastes generated during enrichment are stored in Damar waste dam (Fig. 2). The CT used in the study was supplied with water from the pump going to the Damar waste dam from the Murgul copper plant and dried at 100 ± 5 °C in the oven.

2.2. Materials

Portland cement (PC), CT, NS and MS were used in the study. The specific gravity of PC was found to be 3.13 and the specific surface area (Blaine) as $3316 \text{ cm}^2/\text{g}$. The specific gravity of MS is 2.32 and the specific surface area (BET) is $21.22 \text{ m}^2/\text{g}$. Chemical compositions of PC and MS are presented in Table 1, particle distribution analysis in Fig. 3. The D_{90} , D_{50} and D_{10} values of the PC were found to be $46.265 \mu\text{m}$, $15.404 \mu\text{m}$ and $2.605 \mu\text{m}$, and for MS $426.951 \mu\text{m}$, $117.080 \mu\text{m}$ and $44.162 \mu\text{m}$.

Table 1
Chemical properties of PC and MS

Oxide (%)	CaO	Al ₂ O ₃	Fe ₂ O ₃	SiO ₂	SO ₃	MgO	Na ₂ O	Loss of ignition
PC	63.10	4.41	3.16	19.56	2.99	2.36	0.36	2.70
MS	0.57	1.16	4.24	91.99	0.32	0.76	0.34	1.84

NS tends to agglomerate higher than other pozzolanic materials (Garg et al. 2020). For this reason, the amount of NS used in the study was preferred as 2%. NS mean particle size was 30nm. The surface area was $440 \text{ m}^2/\text{g}$. The mass of the NS in spherical form was $2.2\text{--}2.6 \text{ g}/\text{m}^3$. SEM images of PC, NS and MS are presented in Fig. 4. The mortar mixtures have been prepared with CEN standard sand and mains water.

2.2. Experimental methods

2.2.1. Characterization of CT

Zaleska et al. (2018) argue that only granulometric distribution, chemical composition and strength tests are not sufficient for the characterization of materials to be used instead of cement. He emphasized that if the strength values were lower than expected, the reason could not be found. This situation is attributed to the insufficient analysis of the material (Záleská et al. 2018). For this reason, physical, morphological, chemical, mineralogical, thermo gravimetric and heavy metal content analyzes of CT were performed as the first step in the study. The analyses performed are shown in Fig. 5.

2.2.2. Preparation of mortar samples and tests

12 different mortar mixture has been prepared by substituting of 2% NS, 10% MS, 0%, 5%, 10% and 15% CT instead of cement with the ratio of water/binder (w/b) as 0.50, and aggregate/binder (a/c) as 3. A total of 108 samples were produced with dimensions of $40 \times 40 \times 160 \text{ mm}^3$ (TS EN 196-1 2016). 1350 g of standard sand and 225 g of water were used in all mixtures. The spreading amount of mortars has been

measured (TS EN 1015-3 2000). Binder amounts and mixture codes in the mortar mixture presented in Fig. 6.

The mortar mixtures were removed from the moulds after 24 hours and kept in lime-saturated water at 20 ± 2 °C until the day of the experiment. Ultrasonic Pulse Velocity (UPV) (TS EN 12504-4 2012), flexural and compressive strength tests (TS EN 196-1 2016) were performed on the 2, 7 and 28 days of hardened mortar samples.

Results And Discussion

3.1. Characterization of CT

CT specific gravity is 2.67, the specific surface area is 4953 cm²/g. According to Fig. 7, the cumulative particle distribution of CT is very close to the PC. The material amount of CT below 1 µm is more than PC. PC has a more homogeneous particle distribution than CT. D90, D50 and D10 values of CT are 46.26 µm, 13.79 µm and 0.82 µm. Besides, most of the CT is formed by sharp angular particles as seen from SEM images in Fig. 8.

CT's XRF analysis results are presented in Table 2. It is 91.40% of the sum of SiO₂, Al₂O₃ and Fe₂O₃ in CT. This is above 70% specified by ASTM C 618 – 19 (ASTM C618-19 2019). Oxidized components of CT have been compared with the standard values of cements. This is because the waste material is substituted into cement. An excessive amount of SO₃ in cements causes ettringite formation. For CEM I 42.5 R cement, the SO₃ amount is limited to a maximum of 4.5% (TS EN 196-2 2013). It is seen that the SO₃ level in the CT is below the limit value. MgO in cement should not be more than 5% by mass. (TS EN 197-1 2012). MgO is one of the causes of volume expansion as a result of its reaction with water. In this study, the MgO value is 0.80% and it is below the desired limit value. In the TS EN 196-2 standard for cement, the loss of ignition is specified as 5% at most. CT's loss of ignition was found to be 4.04%. The CT used in this study has been compared with the literature values in recent years (Dandautiya and Singh 2019; Tian et al. 2020; Zhang et al. 2020; Li et al. 2020a; Liu et al. 2020; Jian et al. 2020; Ince et al. 2021). The amount of SiO₂ seems quite high (Fig. 9).

Table 2
Chemical composition of CT

Oxide (%)	SiO ₂	Al ₂ O ₃	Fe ₂ O ₃	CaO	K ₂ O	SO ₃	MgO	TiO ₂	Na ₂ O	Loss of ignition
CT	79.52	7.66	4.22	0.35	1.91	1.11	0.8	0.16	0.11	4.04

According to XRD analysis, the main mineral of CT is SiO₂ (Fig. 10). It is known from the literature that amorphous materials have pozzolanic features (Erdem et al. 2007). However, CT is 87.2% crystalline.

The differential thermogram of the CT showed the most prominent (518 °C and 645 °C) two endothermic reactions. The temperature at which the material begins to decompose is 571 °C, and the temperature at

which decomposition ends is 576 ° C. The amount of decomposed material is calculated as 0.843%. There is little weight loss below 400 ° C. This is an indication that it is a highly pure product with low carbon content (Ludvig et al. 2011). The total weight loss is 4.23% (Fig. 11). TG weight loss and XRF ignition loss values are compatible with each other.

There are studies involving heavy metal analysis around the Damar waste dam and Murgul mine site. Koz et. al. (2012) detected heavy metal concentrations in soils around the Murgul mine (Koz et al. 2012). Yolcubal et. al. (2016) reported that the stream water below the mine was classified as heavily polluted as a result of a leak in the derivation tunnel carrying CT to the waste dam (Yolcubal et al. 2016). Heavy metal contents of CT are presented in Table 3. It is clear that it poses a threat to soil and water, although it is stored in the CT Damar waste dam. It is important to dispose of this waste under appropriate conditions so that it does not pose a potential threat. It is reported that industrial wastes containing heavy metals are successfully disposed of in cement-based composites (Jang et al. 2015; Zhang et al. 2020).

Table 3
The content of heavy metals in CT (mg/kg).

Element	Al	Cd	Cr	Cu	Fe	Mg	Ni	Pb	As
Amount	767	nd*	7.8	57.7	13510	50.2	nd*	nd*	3.9
* nd: Not detected									

3.2. Hardened state properties of mortars

M5 has higher compressive strength at all ages compared to M1 and M9 (Fig. 12 (a)). NS has developed better strength compared to MS. This situation can be explained by the higher SiO₂ content of NS and smaller particle size than MS. It is also known from the literature that NS substitution increases the compressive strength (Garg et al. 2020; Seifan et al. 2020). NS is more effective in pozzolanic reaction with CSH gel than MS (Garg et al. 2020). 2% NS substitution increased compressive strength by 6.84% at day 28 compared to reference cement. M9 mix exhibits lower compressive strength than M1 mix on days 2 and 7, compressive strength higher than M1 mix on day 28. MS strength has a positive effect on older ages. Gleize (2003) has experimentally proved that the compressive strength of mortars with 10% MS is lower than the reference mixture on the 7th day and that the higher strength is obtained compared to the reference on the 28th day (Gleize et al. 2003). In this study, it was determined that 10% MS substitution increased the compressive strength by 4.86% compared to the reference cement (28th day). In terms of chemical effect, as a result of the pozzolanic reaction, the existing gaps in the matrix phase decrease with the conversion of CH to CSH (Güteryüz et al. 2020). The positive effect of only 2% NS on the strength is more than 10% MS. (2017) reported that the carbonation resistance of mortar containing 2% NS was much higher than that of 10% MS (Li et al. 2017). Seifan et al. (2020) emphasized that NS is more promising than MS in improving mechanical properties (Seifan et al. 2020). As the CT substitution amount increases in the mixtures, the compressive strength decreases on the 2nd and 7th days. (Fig. 12

(b)). On the 28th day, it is seen that the highest compressive strength belongs to the M2 mixture. The 5% CT substitution exhibited better compressive strength than the reference. When the compressive strength of mixtures containing NS was examined (Fig. 12 (c)), it was observed that CT substitution reduced compressive strength at all ages. The same situation was observed with mixtures containing MS (Fig. 12 (d)). Especially in M11 and M12 mixtures, it is thought that the reactions required for strength could not occur on the 2nd day due to the decrease in the amount of cement.

The compressive strength of the mixtures has been compared according to the amount of CT they contain. The compressive strength of the samples containing only CT on the 28th day was accepted as 100%, and the varying compressive strengths were calculated with NS and MS substitutions. Figure 13 (a) shows the varying compressive strength of mortars containing 5% CT. While the compressive strength of the M2 mixture was 100%, the compressive strength decreased to 98.89% with NS substitution, and 92.28% with MS substitution. The mixture (M3) containing 10% CT showed similar results when other substitutions were made. Compressive strength decreased to 97.60% with NS substitution (M7) and 93.10% with MS substitution (M11) (Fig. 13 (b)). It is seen that NS and MS substitutions to the mixture containing 15% CT (M4) increase the compressive strength. The compressive strength of the M8 mixture increased to 103.04% and the M12 mixture to 103.67% (Fig. 13 (c)). This situation has been attributed to the pozzolanic feature of NS and MS.

The compressive strengths of the 12 mortar types produced in the study are presented in Fig. 14. On the 2nd day, it was determined that all other mixtures, except for M8, M11 and M12 mixtures, provided the minimum 20MPa strength value in TS EN 196-1 standard. On the 28th day, it is known that the minimum pressure strength stipulated by the standard is 42.5 MPa (TS EN 196-1 2016). Except for M4, M8 and M12 mixtures, all other mortar types provide limit strength. The common feature of M4, M8 and M12 is that they contain 15% CT. This decrease in strength is thought to be due to the decrease in the homogeneity of the cement matrix at the higher CT content (Garg et al. 2020).

As with compressive strength, the higher the amount of CT in all mixes, the lower the flexural strength (Table 4). In addition, the higher the substitution percentage, the higher the strength reduction rate was recorded for PC, NS and MS mixtures. The possible reason for this can be attributed to the poor clamping between CT and aggregate. Unlike the compressive strength, the flexural strength of the M2 mixture on days 2 and 7 increased compared to the M1 mixture. The strength is 1.04% and 3.39% more. This can be attributed to the fact that the flexural strength is more sensitive to changes in the pore structure and the interface transition region between aggregate and cement (Zhang et al. 2019; Nasr et al. 2020). The highest strength value is 8.54 MPa with M5 on the 28th day. This may be due to the development of the strength matrix of NS. Flexural strength decreased by approximately 23.7% for the M12 mixture compared to M1. This result is very close to compressive strength behaviour. It is thought that a 25% reduction in the cement in the mortar matrix causes a decrease in the flexural strength.

Table 4
Flexural strength of mortar mixtures

Mix ID	M1	M2	M3	M4	M5	M6	M7	M8	M9	M10	M11	M12
2-day	5.77	5.83	5.80	4.26	5.76	5.58	5.39	4.26	5.80	5.48	4.44	3.76
7-day	6.78	7.01	6.36	5.64	6.80	6.33	5.98	5.41	6.28	5.87	5.28	5.10
28-day	8.37	8.36	7.82	6.79	8.54	8.04	7.69	6.79	8.10	7.52	6.52	6.39
* ΔR_f	0	0.1	6.6	18.9	-2.0	3.9	8.1	18.9	3.2	10.2	22.1	23.7
* $\Delta R_f = 100 - ((\text{flexural strength of Mx} \times 100) / \text{flexural strength of M1}), x = 2,3,4 \text{ etc. (For 28-day)}$												

UPV values of all mixtures increased due to increasing age (Table 5). It is known from the literature that if the UPV is between 3.5-4.5 km / h, the material quality can be described as "good" (Qasrawi 2000). The material is considered excellent if the UPV is above 4.5 km / h. In this context, it is seen that the 28th day M1, M2, M5 and M6 mixtures can be evaluated as excellent. In this case, it can be said that the homogeneity of the relevant mixtures is better than the other mixtures, and the amount of pores is less compared to other mixtures. When all the mixtures are examined, it can be observed that there is no significant change in the UPV results after the cement has been replaced with CT. This behaviour is since UPV is proportional to the fourth root of compressive strength (Ashish 2018).

Table 5
UPV of mortar mixtures

Mix ID	M1	M2	M3	M4	M5	M6	M7	M8	M9	M10	M11	M12
2-day	4.10	4.15	4.13	4.03	4.15	4.03	4.04	3.91	4.13	3.97	3.88	3.83
7-day	4.48	4.42	4.40	4.27	4.42	4.37	4.38	4.30	4.36	4.25	4.25	4.20
28-day	4.59*	4.53*	4.49	4.38	4.54*	4.55*	4.39	4.37	4.46	4.42	4.08	4.32
Quality: *Excellent (UPV > 4.5 km/s)												

Conclusions And Suggestions

Studies on the usability of the mining industry tailings in cement systems have attracted attention in recent years. In this study, Murgul Copper plant enrichment waste CT was analyzed. In addition, the following results were obtained in line with the experimental findings from CT, CT + NS, CT + MS mortar mixes:

The total content of SiO_2 , Al_2O_3 and Fe_2O_3 in CT is 91.40%. It has been found to have a crystalline structure. The loss of ignition is 4.23% and the particle size distribution is close to cement even though it does not show full homogeneity.

The 5% CT substituted (M2) mixture showed the best compressive strength (49.51 MPa) on day 28 compared to all mixes with reference (M1) and CT substitution. Flexural strength and UPV values also support this result.

CT substitution up to 10% provided the minimum compressive strength required in the standard on the 28th day in mixtures with both NS and MS.

The use of 15% CT instead of cement reduced the compressive strength and flexural strength compared to the reference mixture. However, when used with other wastes such as 15% CT, NS and MS, it has been observed that it is possible to increase the compressive strength of mortar samples compared to mixtures containing only CT.

In mixtures without CT (M1, M5, M9), the highest compressive strength is 52.59 MPa and the flexural strength belongs to the M5 mixture 8.54 with MPa. 2% NS substitute showed better mechanical behaviour than 10% MS substitute.

Waste dams used for the storage of mining tailings need more and more land day by day. The inclusion of CT used in this study by the construction industry will reduce CO_2 emission by using less cement, and will provide an alternative solution step for waste management. In order to evaluate this reserve in future studies, it is recommended to use CT in cement composites with aggregate substitution or to test it in geopolymer production.

Declarations

Availability of data and materials The datasets used and/or analyzed during the current study are available from the corresponding author on reasonable request.

Author contribution İlknur Bekem Kara: conceptualization, methodology, validation, formal analysis, investigation, data curation, writing-original draft, and writing-review and editing.

Funding The author does not receive support from any organization for the submitted work.

Ethics approval The author declares that the manuscript has not been published previously.

Consent to participate Not applicable.

Consent for publication The author consent to the publication of the manuscript.

Competing interests The author declare no competing interests.

References

1. Abhilash PP, Nayak DK, Sangoju B et al (2021) Effect of nano-silica in concrete; a review. *Constr Build Mater* 278:122347
2. Ashish DK (2018) Feasibility of waste marble powder in concrete as partial substitution of cement and sand amalgam for sustainable growth. *J Build Eng* 15:236–242. <https://doi.org/10.1016/j.jobe.2017.11.024>
3. ASTM C618-19 (2019) Standard Specification for Coal Fly Ash and Raw or Calcined Natural Pozzolan for Use in Concrete. ASTM International, West Conshohocken
4. Atmaca N, Abbas ML, Atmaca A (2017) Effects of nano-silica on the gas permeability, durability and mechanical properties of high-strength lightweight concrete. *Constr Build Mater* 147:17–26. <https://doi.org/10.1016/j.conbuildmat.2017.04.156>
5. Bumanis G, Vitola L, Stipniece L et al (2020) Evaluation of Industrial by-products as pozzolans: A road map for use in concrete production. *Case Stud Constr Mater* 13:e00424. <https://doi.org/10.1016/j.cscm.2020.e00424>
6. Choudhary R, Gupta R, Nagar R, Jain A (2021) Mechanical and abrasion resistance performance of silica fume, marble slurry powder, and fly ash amalgamated high strength self-consolidating concrete. *Constr Build Mater* 269:121282. <https://doi.org/10.1016/j.conbuildmat.2020.121282>
7. Dandautiya R, Singh AP (2019) Utilization potential of fly ash and copper tailings in concrete as partial replacement of cement along with life cycle assessment. *Waste Manag* 99:90–101. <https://doi.org/10.1016/j.wasman.2019.08.036>
8. Durgun MY, Sevinç AH (2019) High temperature resistance of concretes with GGBFS, waste glass powder, and colemanite ore wastes after different cooling conditions. *Constr Build Mater* 196:66–81. <https://doi.org/10.1016/j.conbuildmat.2018.11.087>
9. Emamian SA, Eskandari-Naddaf H (2020) Genetic programming based formulation for compressive and flexural strength of cement mortar containing nano and micro silica after freeze and thaw cycles. *Constr Build Mater* 241:118027. <https://doi.org/10.1016/j.conbuildmat.2020.118027>
10. Erdem TK, Meral Ç, Tokyay M, Erdoğan TY (2007) Use of perlite as a pozzolanic addition in producing blended cements. *Cem Concr Compos* 29:13–21. <https://doi.org/10.1016/j.cemconcomp.2006.07.018>
11. Eti Bakır (2021) Murgul Plant. <https://etibakir.com.tr/plants/murgul-plant/?lang=en>. Accessed 16 Feb 2021
12. Garg RR, Garg RR, Bansal M, Aggarwal Y (2020) Experimental study on strength and microstructure of mortar in presence of micro and nano-silica. *Mater Today Proc*. <https://doi.org/10.1016/j.matpr.2020.06.167>
13. Gleize PJP, Müller A, Roman HR (2003) Microstructural investigation of a silica fume-cement-lime mortar. *Cem Concr Compos* 25:171–175. [https://doi.org/10.1016/S0958-9465\(02\)00006-9](https://doi.org/10.1016/S0958-9465(02)00006-9)

14. Güteryüz E, Özen S, Mardani-Aghabaglou (2020) Effect of utilization of mineral admixture on the fresh and hardened properties of air-entrained cement mortars. *Pamukkale Univ J Eng Sci* 26:1053–1061. <https://doi.org/10.5505/pajes.2020.85353>
15. Guo Z, Jiang T, Zhang J et al (2020) Mechanical and durability properties of sustainable self-compacting concrete with recycled concrete aggregate and fly ash, slag and silica fume. *Constr Build Mater* 231:117115. <https://doi.org/10.1016/j.conbuildmat.2019.117115>
16. Horszczaruk E, Aleksandrak M, Cendrowski K et al (2020) Mechanical properties cement based composites modified with nano-Fe₃O₄/SiO₂. *Constr Build Mater* 251:118945. <https://doi.org/10.1016/j.conbuildmat.2020.118945>
17. Ince C, Derogar S, Gurkaya K, Ball RJ (2021) Properties, durability and cost efficiency of cement and hydrated lime mortars reusing copper mine tailings of Lefke-Xeros in Cyprus. *Constr Build Mater* 268:1–17. <https://doi.org/10.1016/j.conbuildmat.2020.121070>
18. International copper study group (2020) *The World Copper Factbook 2020*
19. Jang JG, Ahn YB, Sourì H, Lee HK (2015) A novel eco-friendly porous concrete fabricated with coal ash and geopolymeric binder: Heavy metal leaching characteristics and compressive strength. *Constr Build Mater* 79:173–181. <https://doi.org/10.1016/j.conbuildmat.2015.01.058>
20. Jian S, Gao W, Lv Y et al (2020) Potential utilization of copper tailings in the preparation of low heat cement clinker. *Constr Build Mater* 252:1–9. <https://doi.org/10.1016/j.conbuildmat.2020.119130>
21. Kara C (2020) Effect of High Temperature on Mechanical Properties of Cement Mortar with Nano SiO₂. *Eur J Sci Technol* 247–253. <https://doi.org/10.31590/ejosat.722814>
22. Kara De Maeijer P, Craeye B, Snellings R et al (2020) Effect of ultra-fine fly ash on concrete performance and durability. *Constr Build Mater* 263:120493. <https://doi.org/10.1016/j.conbuildmat.2020.120493>
23. Kooshafar M, Madani H (2020) An investigation on the influence of nano silica morphology on the characteristics of cement composites. *J Build Eng* 30:101293. <https://doi.org/10.1016/j.jobe.2020.101293>
24. Koz B, Cevik U, Akbulut S (2012) Heavy metal analysis around Murgul (Artvin) copper mining area of Turkey using moss and soil. *Ecol Indic* 20:17–23. <https://doi.org/10.1016/j.ecolind.2012.02.002>
25. Lam EJ, Montofré ÍL, Ramírez Y (2021) Mine tailings phytoremediation in arid and semiarid environments. In: *Phytoremediation of Abandoned Mining and Oil Drilling Sites*. Elsevier, pp 115–166
26. Lewis R, Fidjestøl P (2019) Microsilica as an addition. In: *Lea's Chemistry of Cement and Concrete*. Elsevier, pp 509–535
27. Li et al (2020a) Preparation and microstructural characterization of a novel 3D printable building material composed of copper tailings and iron tailings. *Constr Build Mater* 249:118779. <https://doi.org/10.1016/j.conbuildmat.2020.118779>
28. Li H, Ding S, Zhang L et al (2020b) Effects of particle size, crystal phase and surface treatment of nano-TiO₂ on the rheological parameters of cement paste. *Constr Build Mater* 239:117897. <https://doi.org/10.1016/j.conbuildmat.2019.117897>

29. Li LG, Zheng JY, Ng PL, Kwan AKH (2021) Synergistic cementing efficiencies of nano-silica and micro-silica in carbonation resistance and sorptivity of concrete. *J Build Eng* 33:101862. <https://doi.org/10.1016/j.jobe.2020.101862>
30. Li LG, Zhu J, Huang ZH et al (2017) Combined effects of micro-silica and nano-silica on durability of mortar. *Constr Build Mater* 157:337–347. <https://doi.org/10.1016/j.conbuildmat.2017.09.105>
31. Liu S, Wang L, Li Q, Song J (2020) Hydration properties of Portland cement-copper tailing powder composite binder. *Constr Build Mater* 251:1–9. <https://doi.org/10.1016/j.conbuildmat.2020.118882>
32. Ludvig P, Calixto JM, Ladeira LO, Gaspar ICP (2011) Using Converter Dust to Produce Low Cost Cementitious Composites by in situ Carbon Nanotube and Nanofiber Synthesis. *Materials (Basel)* 4:575–584. <https://doi.org/10.3390/ma4030575>
33. Ma C, He J, Qin T et al (2020) A comparison of the influence of micro- and nano-silica on hydration kinetics of Portland cement under different temperatures. *Constr Build Mater* 248:118670. <https://doi.org/10.1016/j.conbuildmat.2020.118670>
34. Mahadevan J, Mani Kuriakose N, Aswath Kannan G et al (2021) Rheological and strength properties of fly ash incorporated rapid hardening cement mix. *Mater Today Proc.* <https://doi.org/10.1016/j.matpr.2020.10.315>
35. Mukharjee BB, Barai SV (2020) Influence of Incorporation of Colloidal Nano-Silica on Behaviour of Concrete. *Iran J Sci Technol - Trans Civ Eng* 44:657–668. <https://doi.org/10.1007/s40996-020-00382-0>
36. Nasr MS, Shubbar AA, Abed ZAAR, Ibrahim MS (2020) Properties of eco-friendly cement mortar contained recycled materials from different sources. *J Build Eng* 31:101444. <https://doi.org/10.1016/j.jobe.2020.101444>
37. Ni C, Wu Q, Yu Z, Shen X (2021) Hydration of Portland cement paste mixed with densified silica fume: From the point of view of fineness. *Constr Build Mater* 272:121906. <https://doi.org/10.1016/j.conbuildmat.2020.121906>
38. Ogawa Y, Uji K, Ueno A, Kawai K (2021) Contribution of fly ash to the strength development of mortars cured at different temperatures. *Constr Build Mater* 276:122191. <https://doi.org/10.1016/j.conbuildmat.2020.122191>
39. Ozturk M, Karaaslan M, Akgol O, Sevim UK (2020) Mechanical and electromagnetic performance of cement based composites containing different replacement levels of ground granulated blast furnace slag, fly ash, silica fume and rice husk ash. *Cem Concr Res* 136:106177. <https://doi.org/10.1016/j.cemconres.2020.106177>
40. Padavala AB, Potharaju M, Kode VR (2021) Mechanical properties of ternary blended mix concrete of fly ash and silica fume. *Mater Today Proc.* <https://doi.org/10.1016/j.matpr.2020.12.127>
41. Qasrawi HY (2000) Concrete strength by combined nondestructive methods simply and reliably predicted. *Cem Concr Res* 30:739–746
42. Qureshi LA, Ali B, Ali A (2020) Combined effects of supplementary cementitious materials (silica fume, GGBS, fly ash and rice husk ash) and steel fiber on the hardened properties of recycled

- aggregate concrete. *Constr Build Mater* 263:120636.
<https://doi.org/10.1016/j.conbuildmat.2020.120636>
43. Sağlam ES, Akçay M (2016) Chemical and mineralogical changes of waste and tailings from the Murgul Cu deposit (Artvin, NE Turkey): implications for occurrence of acid mine drainage. *Environ Sci Pollut Res* 23:6584–6607. <https://doi.org/10.1007/s11356-015-5835-2>
 44. Seifan M, Mendoza S, Berenjian A (2020) Mechanical properties and durability performance of fly ash based mortar containing nano- and micro-silica additives. *Constr Build Mater* 252:119121. <https://doi.org/10.1016/j.conbuildmat.2020.119121>
 45. Sezgin N (2020) Submarine Disposal Method of Mine Tailings (Slurry Sludge). *Nat Hazards Appl Res Cent* 6:209–217. <https://doi.org/10.21324/dacd.544173>
 46. Shafaei D, Yang S, Berlouis L, Minto J (2020) Multiscale pore structure analysis of nano titanium dioxide cement mortar composite. *Mater Today Commun* 22:100779. <https://doi.org/10.1016/j.mtcomm.2019.100779>
 47. Snehal K, Das BB, Akanksha M (2020) Early age, hydration, mechanical and microstructure properties of nano-silica blended cementitious composites. *Constr Build Mater* 233:117212. <https://doi.org/10.1016/j.conbuildmat.2019.117212>
 48. Thomas BS, Damare A, Gupta RC (2013) Strength and durability characteristics of copper tailing concrete. *Constr Build Mater* 48:894–900. <https://doi.org/10.1016/j.conbuildmat.2013.07.075>
 49. Tian X, Zhang H, Zhang T, Fernández CA (2020) Alkali-activated copper tailings-based pastes: Compressive strength and microstructural characterization. *J Mater Res Technol* 9:6557–6567. <https://doi.org/10.1016/j.jmrt.2020.04.043>
 50. Topçu İB, Canbaz M (2008) Effect Of Silica Fume On Mechanic Crack Formations In Concrete. *J Eng Archit Fac Eskişehir Osmangazi Univ* 21:17–26
 51. TS EN 1015-3 (2000) Methods of test for mortar for masonry- Part 3: Determination of consistence of fresh mortar (by flow table). Turkish Standard Institute, Ankara, Turkey
 52. TS EN 12504-4 (2012) Testing concrete - Part 4: Determination of ultrasonic pulse velocity. Turkish Standard Institute, Ankara, Turkey
 53. TS EN 196-1 (2016) Methods of testing cement - Part 1: Determination of strength. Turkish Standard Institute, Ankara, Turkey
 54. TS EN 196-2 (2013) Methods of testing cement - Part 2: Chemical analysis of cement. Turkish Standard Institute, Ankara, Turkey
 55. TS EN 197-1 (2012) Cement - Part 1: Composition, specifications and conformity criteria for common cements. Turkish Standard Institute, Ankara, Turkey
 56. Vargas F, Lopez M, Rigamonti L (2020) Environmental impacts evaluation of treated copper tailings as supplementary cementitious materials. *Resour Conserv Recycl* 160:104890. <https://doi.org/10.1016/j.resconrec.2020.104890>

57. Xu W, Zhang Y, Zuo X, Hong M (2020) Time-dependent rheological and mechanical properties of silica fume modified cemented tailings backfill in low temperature environment. *Cem Concr Compos* 114:103804. <https://doi.org/10.1016/j.cemconcomp.2020.103804>
58. Yiğit B, Salihoğlu G, Mardani-Aghabaglou A et al (2020) Atıksu arıtma çamurlarının yakılmasıyla oluşan küllerin yapı malzemesi olarak geri kazanımı. *Gazi Üniversitesi Mühendislik-Mimarlık Fakültesi Derg* 35:1647–1664. <https://doi.org/10.17341/gazimmfd.544678>
59. Yolcubal I, Demiray AD, Çiftçi E, Sanğu E (2016) Environmental impact of mining activities on surface water and sediment qualities around Murgul copper mine, Northeastern Turkey. *Environ Earth Sci* 75:1–25. <https://doi.org/10.1007/s12665-016-6224-y>
60. Yu J, Zhang M, Li G et al (2020) Using nano-silica to improve mechanical and fracture properties of fiber-reinforced high-volume fly ash cement mortar. *Constr Build Mater* 239:117853. <https://doi.org/10.1016/j.conbuildmat.2019.117853>
61. Záleská M, Pavlíková M, Pavlík Z et al (2018) Physical and chemical characterization of technogenic pozzolans for the application in blended cements. *Constr Build Mater* 160:106–116. <https://doi.org/10.1016/j.conbuildmat.2017.11.021>
62. Zhang H, Ji T, He B, He L (2019) Performance of ultra-high performance concrete (UHPC) with cement partially replaced by ground granite powder (GGP) under different curing conditions. *Constr Build Mater* 213:469–482. <https://doi.org/10.1016/j.conbuildmat.2019.04.058>
63. Zhang Y, Shen W, Wu M et al (2020) Experimental study on the utilization of copper tailing as micronized sand to prepare high performance concrete. *Constr Build Mater* 244:118312. <https://doi.org/10.1016/j.conbuildmat.2020.118312>

Figures



Figure 1

Location map of the study area (Sağlam and Akçay 2016).



Figure 2

Murgul copper plant and Damar waste dam

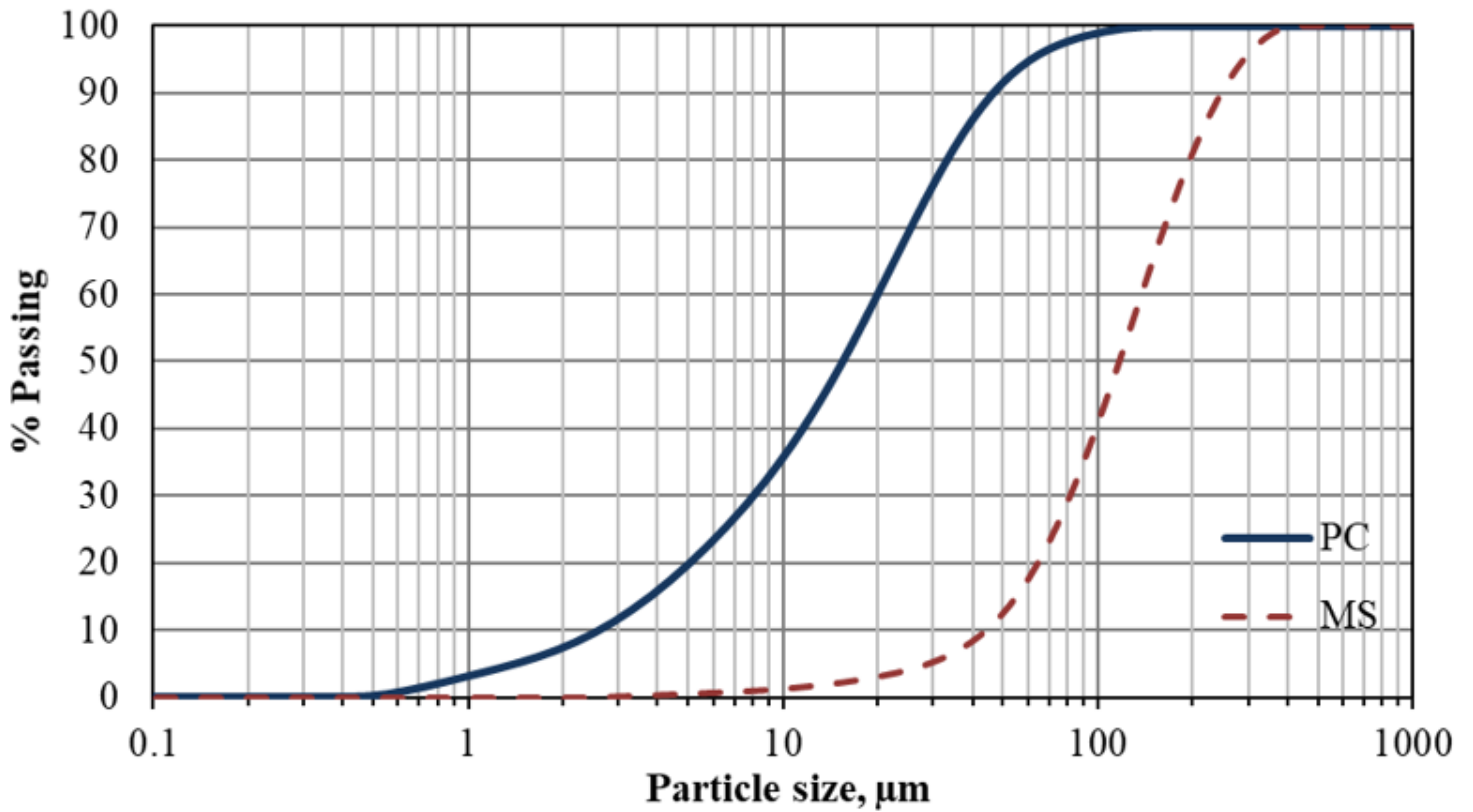


Figure 3

The particle size distribution of PC and MS

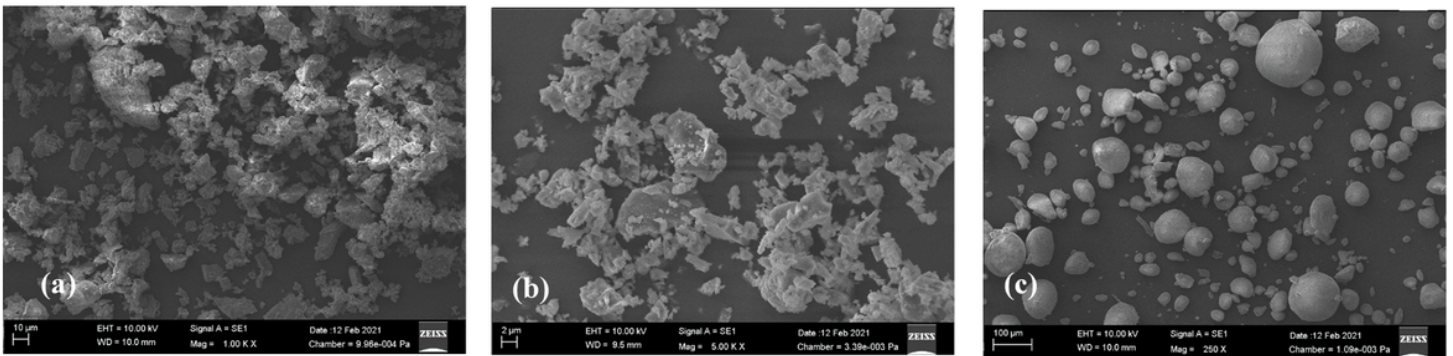


Figure 4

The morphology of (a) PC magnifications 1000X, (b) NS magnifications 5000X, and (c) MS magnifications 1000X

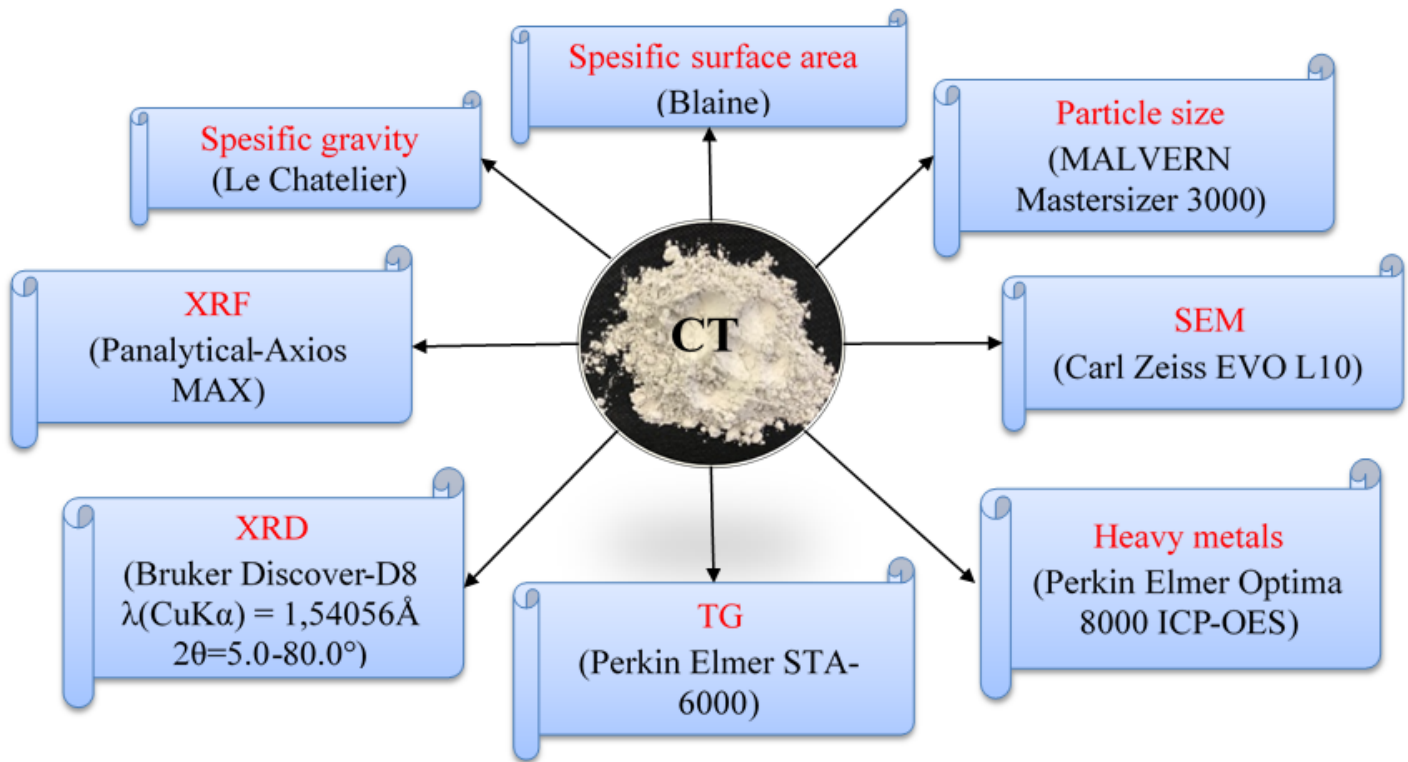


Figure 5

CT analyses

Mix code	Proportion of binders	PC (g)	CT (g)	NS (g)	MS (g)	Flow (mm)
M1	100% PC	450.0				155
M2	95%PC + 5%CT	427.5	22.5			153
M3	90%PC + 10%CT	405.0	45.0			142
M4	85%PC + 15%CT	382.5	67.5			140
M5	98%PC + 2%NS	441.0		9.0		155
M6	93%PC + 5%CT + 2%NS	418.5	22.5	9.0		153
M7	88%PC + 10%CT + 2%NS	396.0	45.0	9.0		148
M8	83%PC + 15%CT + 2%NS	373.5	67.5	9.0		130
M9	90%PC + 10%SF	405.0			45.0	136
M10	85%PC + 5%CT + 10%SF	382.5	22.5		45.0	129
M11	80%PC + 10%CT + 10%SF	360.0	45.0		45.0	125
M12	75%PC + 15%CT + 10%SF	337.5	67.5		45.0	120

Figure 6

Quantity of materials used in mortar mixes

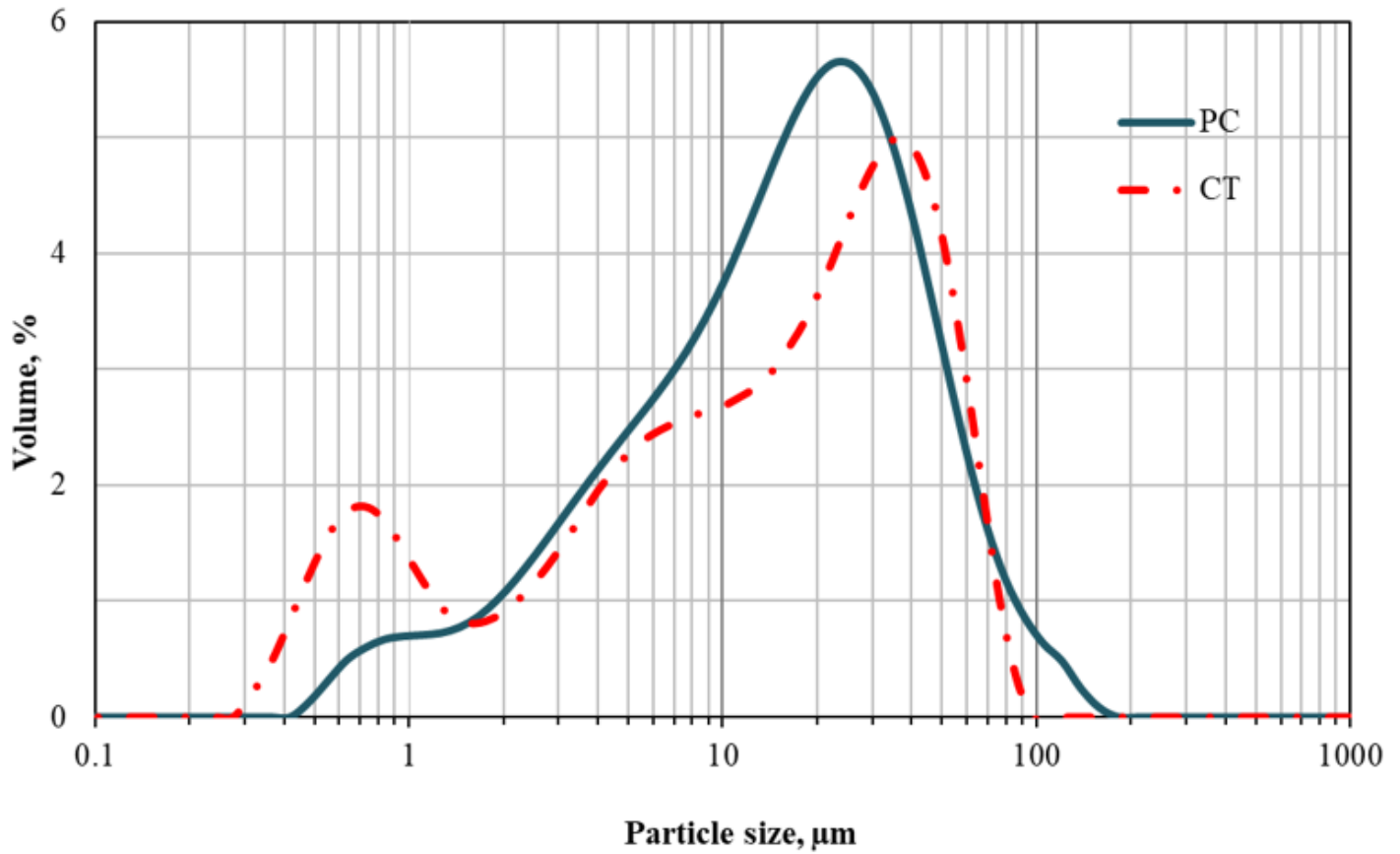


Figure 7

The cumulative particle size distribution of PC and CT

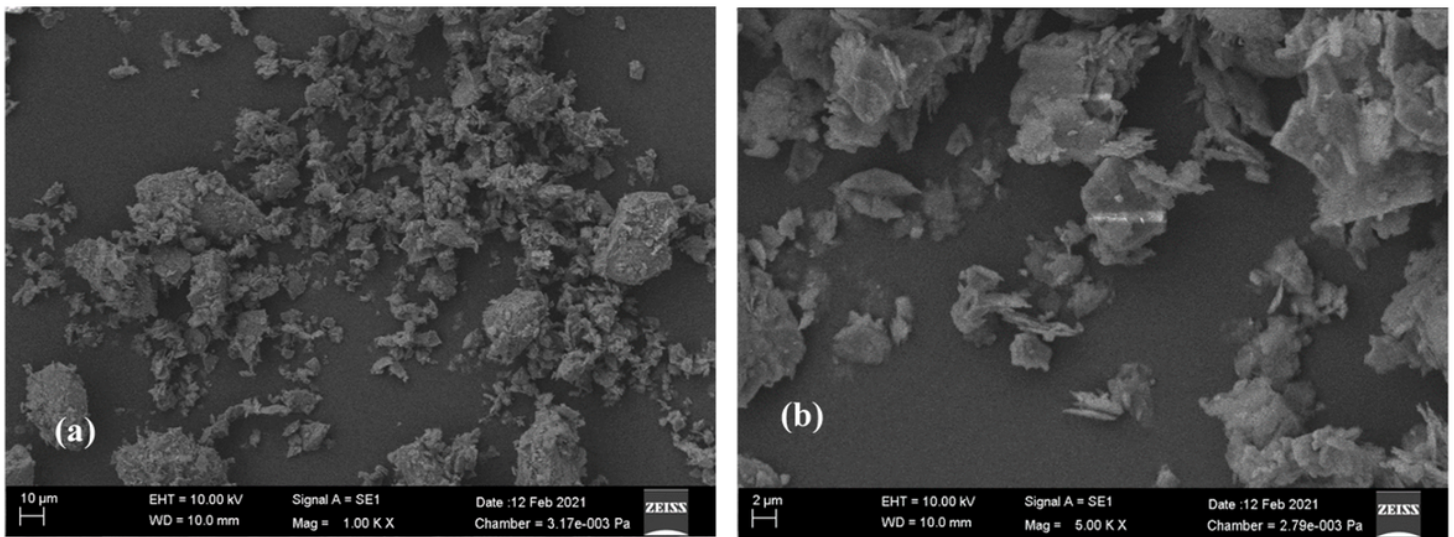


Figure 8

The morphology of CT particles at 1000X (a) and 5000X (b) magnifications

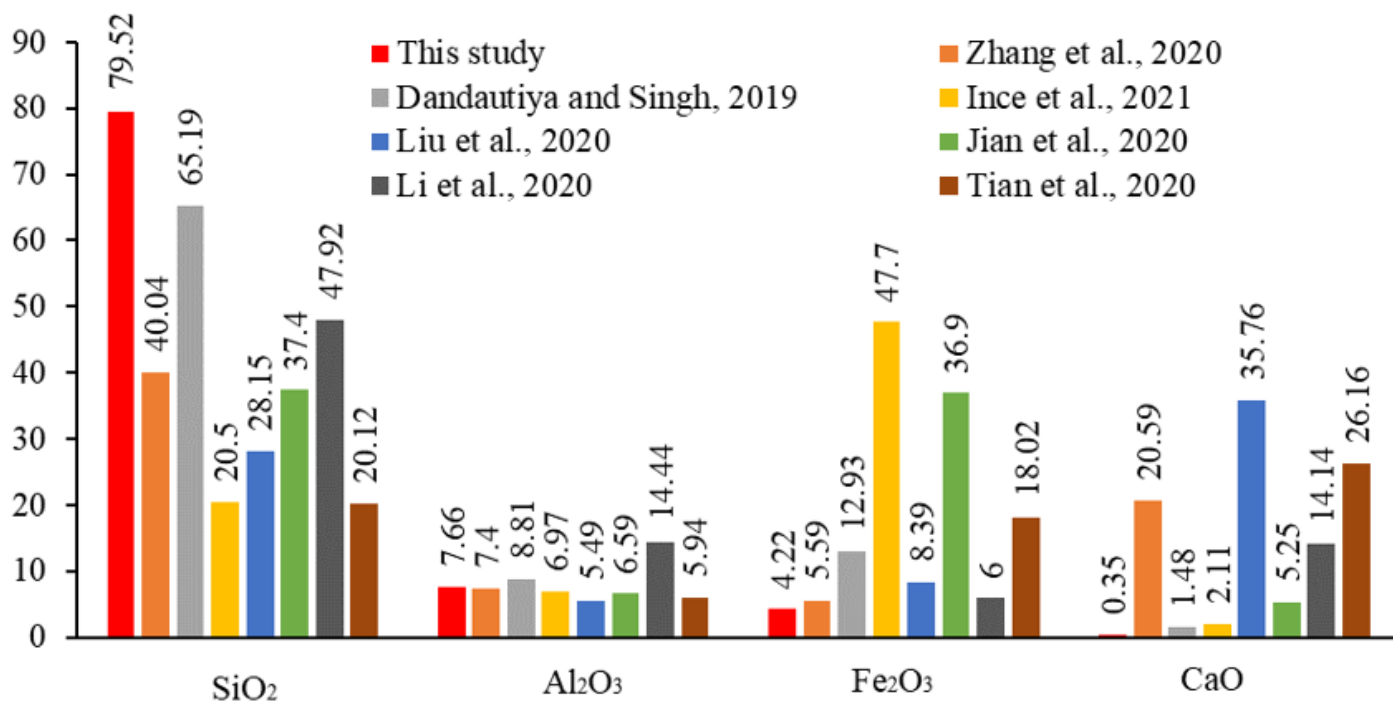


Figure 9

Main chemical composition of CT in this study and literature.

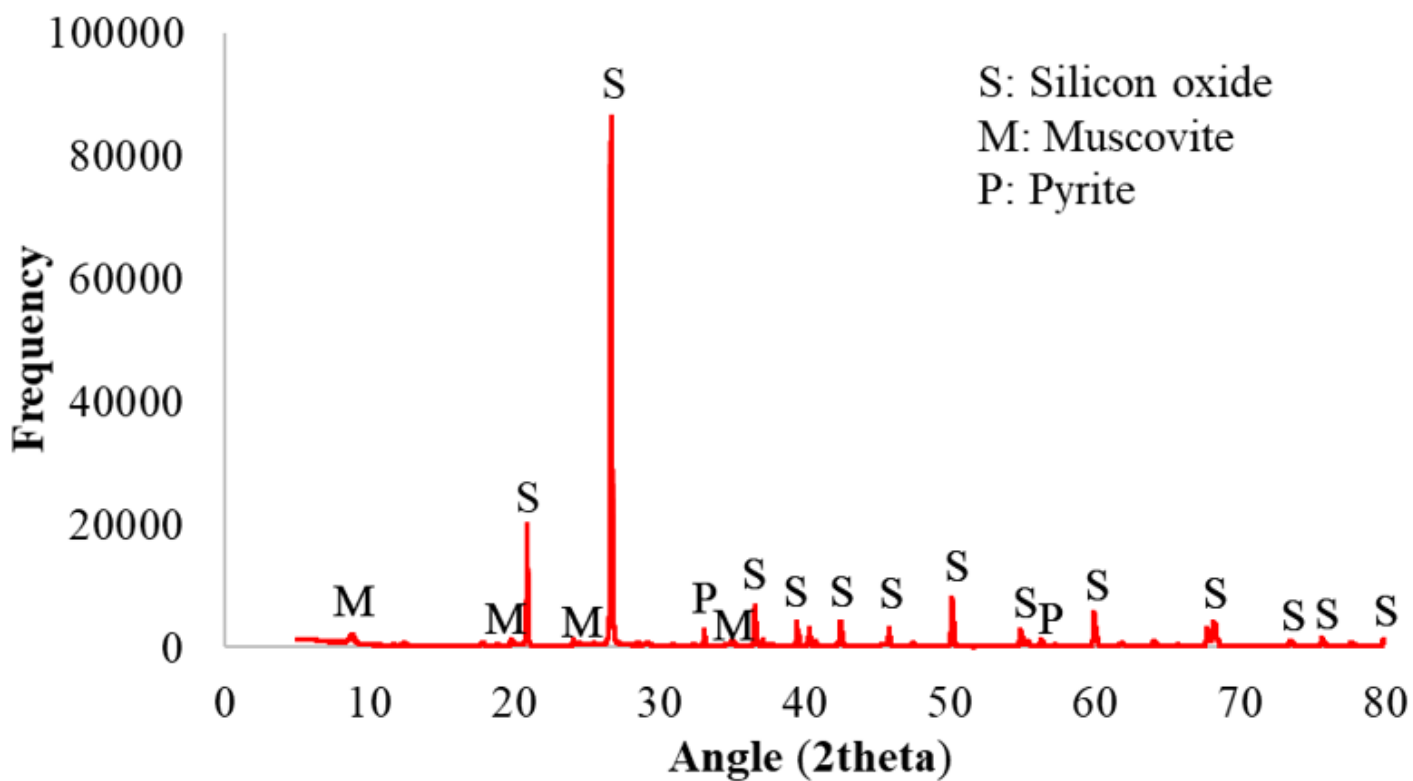


Figure 10

XRD patterns of CT

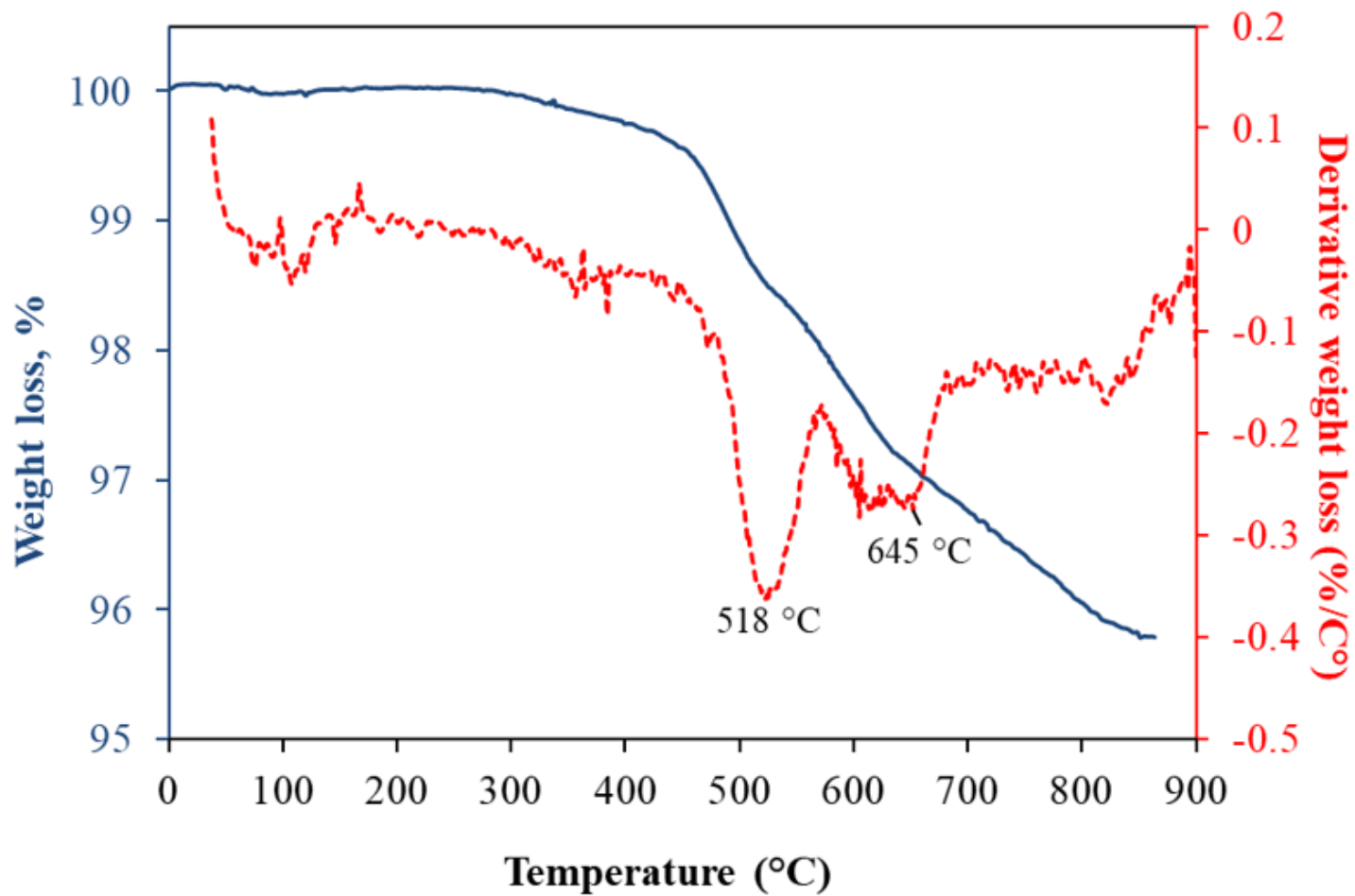


Figure 11

TG analysis

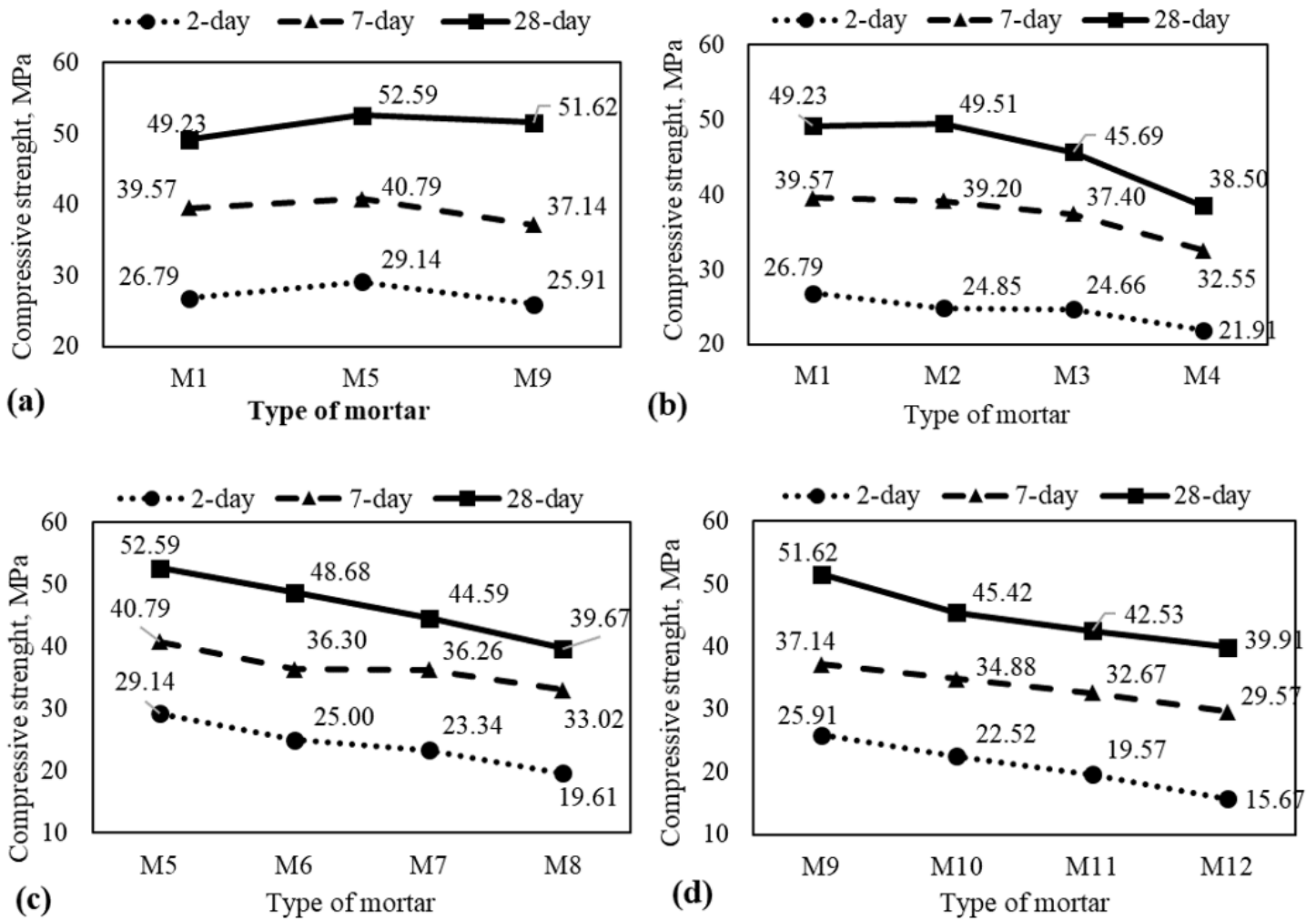


Figure 12

Compressive strength of (a) mixtures not including CT , (b) PC+CT mixtures, (c) PC+CT+NS mixtures, (d) PC+CT+MS mixtures

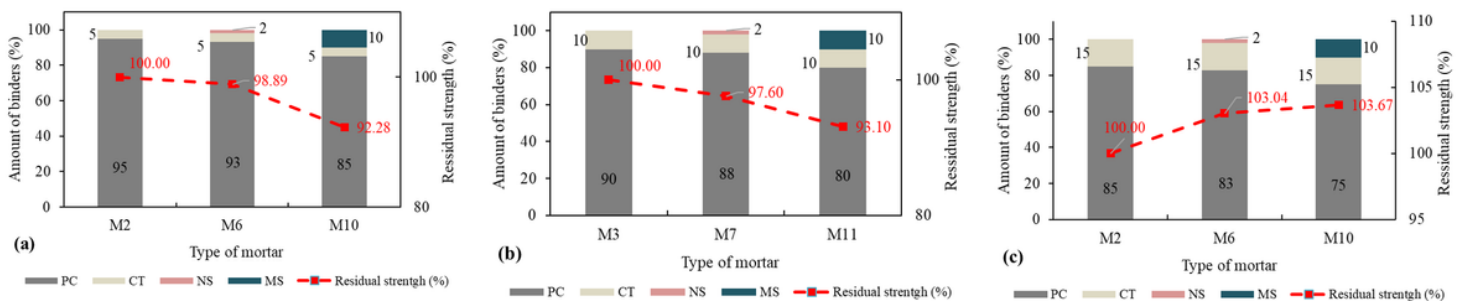


Figure 13

Residual strength of (a) Mixtures containing 5% CT, (b) Mixtures containing 10% CT, (c) Mixtures containing 15% CT

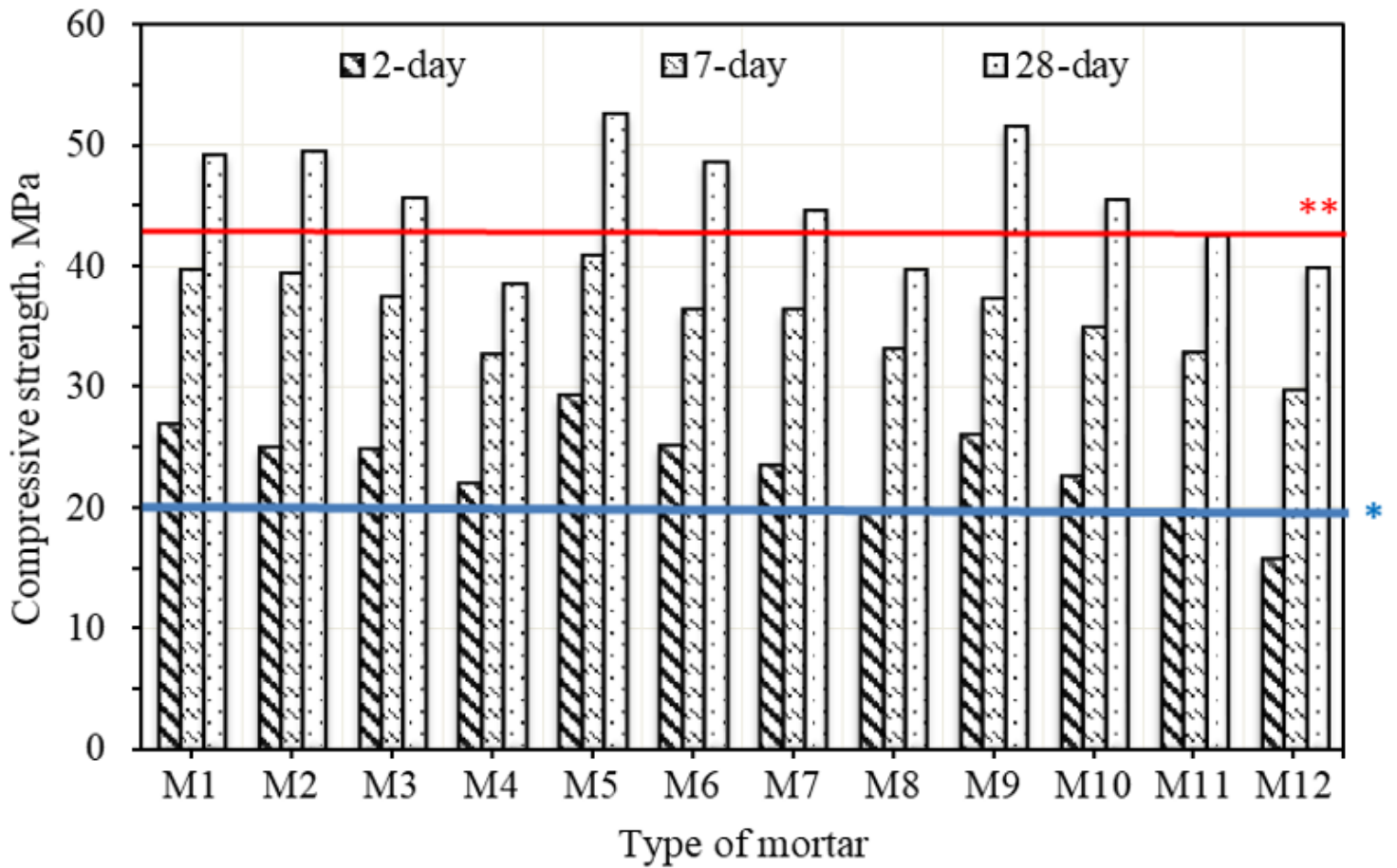


Figure 14

Compressive strength of mortar mixtures (*TSEN 197-1 limit ≥ 20.0 MPa at 2-day) **TSEN 197-1 limit ≥ 42.5 MPa at 28-day)

Supplementary Files

This is a list of supplementary files associated with this preprint. Click to download.

- [Graphicalabstract..docx](#)